

# IL-22-STAT3 Pathway Plays a Key Role in the Maintenance of Ileal Homeostasis in Mice Lacking Secreted Mucus Barrier

Bruno Sovran, MSc,<sup>\*,†</sup> Linda M. P. Loonen, PhD,<sup>\*,†</sup> Peng Lu, PhD,<sup>‡,§</sup> Floor Hugenholtz, MSc,<sup>\*,||</sup> Clara Belzer, PhD,<sup>\*,||</sup> Ellen H. Stolte, PhD,<sup>†</sup> Mark V. Boekschoten, PhD,<sup>\*,¶</sup> Peter van Baarlen, PhD,<sup>†</sup> Michiel Kleerebezem, PhD,<sup>\*,†,\*\*</sup> Paul de Vos, PhD,<sup>\*,††</sup> Jan Dekker, PhD,<sup>\*</sup> Ingrid B. Renes, PhD,<sup>‡,##</sup> and Jerry M. Wells, PhD<sup>\*,†</sup>

**Background:** Muc2-deficient mice show no signs of ileal pathology but the mechanisms remained unknown.

**Methods:** Wild-type (WT), Muc2<sup>+/-</sup>, and Muc2<sup>-/-</sup> mice were killed at 2, 4, and 8 weeks of age. Total RNA from ileum was used for full genome transcriptome analysis and qPCR. Microbiota composition was determined using a mouse intestinal chip (MITChip). Morphological and immunohistochemical studies were performed on segments of ileum.

**Results:** The ileum was colonized by more diverse microbiota in young (week 4) WT than in Muc2<sup>-/-</sup> mice, and composition was influenced by genotype. Weaning was associated with major changes in the transcriptome of all mice, and the highest number of differentially expressed genes compared with adults, reflecting temporal changes in microbiota. Although the spatial compartmentalization of bacteria was compromised in Muc2<sup>-/-</sup> mice, gene set enrichment analysis revealed a downregulation of Toll-like receptor, immune, and chemokine signaling pathways compared to WT mice. The predicted effects of enhanced IL-22 signaling were identified in the Muc2<sup>-/-</sup> transcriptome as the upregulation of epithelial cell proliferation altered expression of mitosis and cell-cycle control pathways. This is consistent with increased villus length and number of Ki67<sup>+</sup> epithelial cells in Muc2<sup>-/-</sup> mice. Additionally, expression of the network of IL-22 regulated defense genes, including Fut2, Reg3β, Reg3γ, Relmb, and the Defensin Defb46 were increased in Muc2<sup>-/-</sup> mice.

**Conclusions:** These findings highlight a role for the IL-22-STAT3 pathway in maintaining ileal homeostasis when the mucus barrier is compromised and its potential as a target for novel therapeutic strategies in inflammatory bowel disease.

(*Inflamm Bowel Dis* 2015;21:531–542)

**Key Words:** Muc2, Reg3 proteins, intestinal homeostasis, ileum, microbiota, interleukin 22

Secreted mucus, antimicrobial proteins, and immunoglobulin A in the lumen play a key role in maintaining intestinal homeostasis by regulating contact between host cells and potentially harmful antigens and microbes.<sup>1,2</sup> Intestinal mucus is primarily

composed of mucin 2 (Muc2), secreted by goblet cells in the epithelium.<sup>3,4</sup> Glycans of Muc2 were recently shown to confer tolerogenic properties to lamina propria (LP) dendritic cells (DCs) through interaction with a galectin 3-dectin 1-FcγRIIB receptor complex.<sup>5</sup> Muc2 also enhances epithelial expression of B-cell cytokines and trypsin-like serine protease, promoting development of tolerogenic DCs and anti-inflammatory mechanisms contributing to gut homeostasis, possibly through the same receptor complex.<sup>5</sup> Mouse colonic mucus is composed of an inner layer, attached to the epithelium and largely devoid of bacteria, and a less-dense outer layer, containing commensal bacteria and luminal contents.<sup>6</sup> Both mucus sublayers have essentially the same composition, suggesting the outer layer arises from limited specific proteolytic cleavage and volumetric expansion of the inner layer in combination with (partial) consumption by bacteria.<sup>7</sup> The density and stratified organization of the inner mucus layer is proposed to prevent penetration by bacteria, minimizing contact of bacteria and ingesta with the epithelium. The structure and function of small intestinal mucus is less well understood, and it is noticeably thinner than in the colon.<sup>6</sup>

Defects in barrier properties of mucus are considered to be contributing factors in patients with inflammatory bowel disease (IBD) with Crohn's disease or ulcerative colitis. In both forms of IBD,

Received for publication October 17, 2014; Accepted November 18, 2014.

From the \*Top Institute Food and Nutrition, Wageningen, the Netherlands; †Host-Microbe Interactomics Group, Animal Sciences Department, Wageningen University and Research Center, Wageningen, the Netherlands; ‡Department of Pediatrics, Erasmus MC-Sophia, Rotterdam, the Netherlands; §Department of Pediatrics, Academic Medical Center, Amsterdam, the Netherlands; ||Department of Agrotechnology and Food Sciences, Laboratory of Microbiology, Wageningen University and Research Center, Wageningen, the Netherlands; ¶Department of Agrotechnology and Food Sciences, Division of Human Nutrition, Wageningen University and Research Center, Wageningen, the Netherlands; \*\*NIZO food research, Ede, the Netherlands; ††University Medical Center of Groningen, Groningen, the Netherlands; and ‡‡Nutricia Research, Utrecht, the Netherlands.

Supported by TI Food and Nutrition, a public-private partnership on precompetitive research in food and nutrition. The public partners are responsible for the study design, data collection and analysis, decision to publish, and preparation of the manuscript. The private partners have contributed to the project through regular discussion.

The authors have no conflicts of interest to disclose.

Reprints: Jerry M. Wells, PhD, PO Box 338, 6700 AH Wageningen, the Netherlands (e-mail: jerry.wells@wur.nl).

Copyright © 2015 Crohn's & Colitis Foundation of America, Inc.

DOI 10.1097/MIB.0000000000000319

Published online 29 January 2015.

the intestinal mucus harbors higher numbers of bacteria than healthy subjects<sup>8</sup> and in patients with ulcerative colitis, the colonic mucus layer is thinner, with a 70% reduction of Muc2 production in active periods of disease.<sup>9,10</sup> Recently, colonic mucus in an experimental rodent model of colitis and in biopsy samples from patients with ulcerative colitis seemed highly penetrable to fluorescent beads compared with healthy tissue.<sup>11</sup> The diminished barrier functionality of mucus in colitis may be due to structural changes in the sulfation and sialylation of Muc2 oligosaccharides, as was reported in IBD patients.<sup>12</sup> A consequence of defective barrier function is increased contact of bacteria with the epithelium, which triggers inflammatory responses through recognition of microbe-associated molecular patterns, by pattern recognition receptors of the innate immune system, including Toll-like receptors and NOD-like receptors, resulting in inflammatory mucosal cytokine production and increased epithelial permeability.<sup>13</sup> In IBD, a dysfunctional mucus barrier will increase influx of luminal antigens into the LP, leading to innate and adaptive responses to luminal antigens and a perpetuating cycle of inflammation and barrier dysfunction that may be difficult to resolve without therapy.<sup>14</sup>

An abnormal composition and decreased diversity of (specific subgroups of) the microbiota is associated with chronic inflammatory conditions, such as IBD.<sup>14,15</sup> This may be due to the selective targeting of members of the resident microbiota by antimicrobial factors induced by the host inflammatory response, leading to increased abundance of potentially pathogenic bacterial pathogens in the microbiota.<sup>13</sup>

Muc2<sup>-/-</sup> mice lack an intestinal mucus layer and develop spontaneous colitis from 4 weeks of age onwards.<sup>16</sup> In these mice, bacteria are found in colonic crypts and in direct contact with epithelial cells.<sup>6</sup> The inflammatory responses in Muc2<sup>-/-</sup> mice before development of colitis have been previously studied in the colon of 2- and 4-week-old mice.<sup>17,18</sup> Distinct phases were observed in colitis development, which might be related to the expansion of the microbiota after weaning and/or loss of protective factors in mother's milk. The most notable changes observed in Muc2<sup>-/-</sup> mice were the exacerbation of inflammatory gene expression after weaning and a decline in the number of regulatory T cells.<sup>17</sup> None of the previous studies in Muc2<sup>-/-</sup> mice have deeply investigated the effects of Muc2-deficiency in the ileum. Here, we performed transcriptomics, histology, and 16S microbiota profiling on ileal samples from wild-type (WT), Muc2<sup>-/-</sup>, and Muc2<sup>+/-</sup> mice at 2, 4, and 8 weeks after birth with the aim of gaining a better understanding of homeostatic mechanisms, early indicators of gut barrier dysfunction, and the impact of mucus on diversity and composition of microbiota in the ileum.

## MATERIALS AND METHODS

### Animals

Muc2<sup>-/-</sup> mice with a 129SV background were bred as previously described.<sup>19</sup> Mice were generated from interbreeding Muc2<sup>+/-</sup> mice and genotyped.<sup>19</sup> Mice were housed in a specific

pathogen-free environment with ad libitum access to AIN93 diet (Special Diets Services, Witham, Essex, United Kingdom) and acidified tap water in a 12-hour light/dark cycle. The Erasmus MC Animal Ethics Committee (Rotterdam, the Netherlands) approved the animal experiments.

### Experimental Set up

Groups of WT, Muc2<sup>+/-</sup>, and Muc2<sup>-/-</sup> (n = 5 in each group) littermates were housed together with their respective birth mothers until weaning at 21 days and killed at 14, 28, and 56 days postnatal. Ileal tissues were excised and fixed in 4% (wt/vol) paraformaldehyde in phosphate-buffered saline (PBS), stored in RNAlater (Qiagen, Venlo, the Netherlands) at -20°C or frozen in liquid nitrogen and stored at -80°C. Additionally, colonic tissue was collected, fixed in 4% paraformaldehyde in PBS and embedded in paraffin.

### Histology

Paraffin sections (5 μm) of ileum were attached to poly-L-lysine-coated glass slides (Thermo Fisher Scientific, Dreieich, Germany). After overnight incubation at 37°C, slides were dewaxed and hydrated stepwise using 100% xylene followed by several solutions of distilled water containing decreasing amounts of ethanol. Sections were stained with hematoxylin and eosin (H&E) and Periodic Acid Schiff (PAS)/Alcian blue.<sup>20</sup> Ten morphologically well-oriented crypt-villus regions were randomly chosen per ileal segment, and their length was measured using ImageJ software (National Institutes of Health, Bethesda, MD).

### Immunohistochemistry

The slides were deparaffinized, and antigen retrieval was performed by heating the sections for 20 minutes in 0.01 M sodium citrate (pH 6.0) at 100°C. Sections were washed for 3 hours with 3 changes of PBS. Nonspecific binding was reduced using 10% (vol/vol) goat serum (Invitrogen, Life Technologies Ltd., Paisley, United Kingdom) in PBS for 30 minutes at room temperature. Cell proliferation marker Ki67 was detected by incubating the sections with anti-Ki67 antibody (Abcam, Cambridge, United Kingdom) diluted 1:200 in PBS, 90 minutes at room temperature. Apoptotic cells were identified by staining for cleaved-Caspase 3 expression using an anti-Caspase-3 antibody (Abcam) diluted 1:200 in PBS, overnight at 4°C.

### Detection of Bacteria Using Fluorescence In Situ Hybridization

The slides were deparaffinized with xylene and washed twice in 100% ethanol. The tissue sections were incubated with the universal bacterial probe EUB338 (5'-GCTGCTCCCGTAG-GAGT-3') (Isogen Bioscience BV, De Meern, the Netherlands) conjugated to Alexa Fluor 488. A "non-sense" probe (5'-CGACG-GAGGGCATCTCA-3'), conjugated to Cy3, was used as a negative control. Tissue sections were incubated overnight with 0.5 μg of probe in 50 μL of hybridization solution (20 mmol/L Tris-HCl [pH 7.4], 0.9 mol/L NaCl, 0.1% [wt/vol] SDS) at 50°C in a humid environment using a coverslip to prevent drying of the sample. The sections were washed with (20 mmol/L Tris-HCl [pH 7.4], 0.9 mol/L NaCl) at 50°C for 20 minutes and then washed

2 times in PBS for 10 minutes in the dark and incubated with DRAQ5 (Invitrogen) (1:1000) for 1 hour at 4°C to stain nuclei. Sections were washed 2 times in PBS for 10 minutes, mounted in fluoromount G (SouthernBiotech, Birmingham, AL) and stored at 4°C.

### RNA Isolation, cDNA Synthesis, and qPCR

Total RNA was isolated using the RNeasy kit (Qiagen) with a DNase digestion step according to the manufacturer's protocol. One microgram of RNA was reverse transcribed using a qScript cDNA synthesis kit (Quanta Biosciences, Gaithersburg, MD) according to the manufacturer's protocol. QPCR was performed on a Rotorgene 2000 real-time cycler (Qiagen) (Table 1 for qPCR primer sequences). For qPCR 5  $\mu$ L cDNA (1:20 diluted from cDNA synthesis mixture) was used, together with 300 nmol/L forward and reverse primer, 6.25  $\mu$ L 2 $\times$  Rotor-Gene SYBR Green PCR kit (Qiagen) and demineralized water up to a volume of 12.5  $\mu$ L. QPCR was performed (2 minutes 95°C, 40 cycles of 15 seconds at 95°C, 1 minute at 60°C, and 2 minutes at 60°C) on a Rotorgene 2000 real-time cycler (Qiagen).

Raw QPCR data were analyzed using Rotorgene Analysis Software V5.0 (Qiagen, Hilden, Germany). Changes in transcript levels were calculated relative to the glyceraldehyde-3-phosphate dehydrogenase (Gapdh) and hypoxanthine phosphoribosyl transferase (Hprt) genes that were expressed at the same level in WT, Muc2<sup>+/-</sup>, and Muc2<sup>-/-</sup> mice. Reactions lacking reverse transcriptase or template were included as controls in all experiments, and no amplification above background levels was observed. The melting temperature and profile of each melting curve was checked to ensure specificity of the amplification product. For each polymerase chain reaction, amplification of the correct amplicon was verified by sequencing.

Statistics were performed using GraphPad Prism 5.0 software (GraphPad, San Diego, CA). Data shown are the mean values and the standard error of the mean, analyzed with the nonparametric Mann-Whitney test. Differences were considered statistically significant when  $P < 0.05$ .

### Transcriptome Analysis

Quantity and quality of ileal RNA (5 arrays of individual mice per group) was assessed using spectrophotometry (ND-1000;

NanoDrop Technologies, Wilmington, NC) and Bionalyzer 2100 (Agilent, Santa Clara, CA), respectively. RNA was only used to generate cDNA and perform microarray hybridization when there was no evidence of RNA degradation (RNA Integrity Number >8). One hundred nanogram of total RNA was labeled using the Ambion WT Expression kit (Life Technologies Ltd, Paisley, United Kingdom) together with the Affymetrix GeneChip WT Terminal Labeling kit (Affymetrix, Santa Clara, CA). Labeled samples were hybridized to Affymetrix GeneChip Mouse Gene 1.1 ST arrays. Hybridization, washing, and scanning of the array plates were performed on an Affymetrix GeneTitan Instrument, according to the manufacturer's recommendations.

Quality control of the data sets obtained from the scanned Affymetrix arrays was performed using Bioconductor<sup>21</sup> packages integrated in an online pipeline.<sup>22</sup> Probe sets were redefined according to Dai et al<sup>23</sup> using current genome information. In this study, probes were reorganized based on the Entrez Gene database (remapped CDF v14.1.1). Normalized expression estimates were obtained from the raw intensity values using the Robust Multiarray Analysis preprocessing algorithm available in the Bioconductor library affyPLM using default settings.<sup>24</sup>

Differentially expressed probe sets were identified using linear models, applying moderated T-statistics that implemented empirical Bayes regularization of SEs.<sup>25</sup> A Bayesian hierarchical model was used to define an intensity-based moderated T-statistic, which takes into account the degree of independence of variances relative to the degree of identity and the relationship between variance and signal intensity.<sup>26</sup> Only probe sets with a fold change of at least 1.2 (up/down) and  $P$  value <0.05 were considered to be significantly different. Pathway analysis was performed by Gene Set Enrichment Analysis (GSEA)<sup>27,28</sup> and visualized in Cytoscape (<http://www.ncbi.nlm.nih.gov/pubmed/20656902>).

### Bacterial DNA Extraction and Microbiota Profiling

Except for 2-week-old mice, which appeared to lack sufficient luminal content to allow sampling, the contents of the

**TABLE 1.** Quantitative PCR Primer Sequences (5' to 3', Left to Right)

	Forward Primer	Reverse Primer
Gapdh	GGTGAAGGTCGGTGTGAAC	CTCGCTCCTGGAAGATGGTG
Hprt	GTTAAGCAGTACAGCCCCAAA	AGGGCATATCCAACAACAAACTT
Muc2	ACCTGGGGTGACTTCCA	CCTTGGTGTAGGCATCGTTC
Reg3 $\gamma$	TTCCTGTCTCCATGATCAAAA	CATCCACCTCTGTTGGGTTCA
Reg3	ATGCTGCTCTCCTGCCTGATG	CTAATGCGTGCGGAGGGTATATTC
Fut2	AGTCTTCGTGGTTACAAGCAAC	TGGCTGGTGAGCCCTCAATA
IL-1 $\beta$	AGTTGACGGACCCCAAAAG	CACGGGAAAGACACAGGTAG

FUT2, fucosyltransferase 2; Gapdh, glyceraldehyde 3-phosphate dehydrogenase; Hprt, hypoxanthine guanine phosphoribosyl transferase; IL-1 $\beta$ , interleukin-1 $\beta$ ; Muc2, mucin 2; Reg3 $\gamma$ , regenerating islet-derived protein 3 gamma.

ileum could be recovered by gently squeezing and the DNA was extracted using PowerSoil DNA extraction kit (MO BIO Laboratories, Carlsbad, CA). Microbiota composition was analyzed by Mouse Intestinal Tract Chip (MITChip), a diagnostic 16S rRNA array that consists of 3580 unique probes especially designed to profile mouse intestine microbiota.<sup>29</sup> 16S rRNA gene amplification, in vitro transcription and labeling, and hybridization were carried out as described previously.<sup>30</sup> The data were normalized and analyzed using a set of R-based scripts in combination with a custom-designed relational database, which operates under the MySQL database management system. For the microbial profiling, the Robust Probabilistic Averaging signal intensities of 2667 specific probes for the 94 genus-level bacterial groups detected on the MITChip were used.<sup>31</sup> Diversity calculations were performed using a microbiome R-script package (<https://github.com/microbiome>). Multivariate statistics, redundancy analysis, and principal response curves were performed in Canoco 5.0 and visualized in triplots or a principal response curves plot.<sup>32</sup>

### Ethical Considerations

Animal care and procedures were in compliance with the guidelines of the Animal Ethics Committee, Erasmus MC (Rotterdam, the Netherlands).

## RESULTS

### Muc2<sup>-/-</sup> Mice Lack Secreted Mucus and Muc2-positive Goblet Cells

From 4 weeks of age, colitis was observed in proximal colon in Muc2<sup>-/-</sup> mice (Fig. 1A). Alcian blue staining was used to identify acidic carbohydrates like Muc2 and PAS for neutral carbohydrates. PAS-positive and combined PAS-Alcian blue-positive goblet cells were observed in the ileum of WT and Muc2<sup>+/-</sup> mice. In contrast, goblet cells in Muc2<sup>-/-</sup> mice only stained positive for PAS (Fig. 1B).

Immunohistochemistry revealed the presence of Muc2-positive goblet cells in WT and Muc2<sup>+/-</sup> mice, and the absence of such cells in Muc2<sup>-/-</sup> mice (Fig. 1B). Ileal Muc2 messenger RNA (mRNA) expression was absent in Muc2<sup>-/-</sup> mice but was not significantly different between WT and Muc2<sup>+/-</sup> (Fig. 1C). Similar numbers of Muc2-stained goblet cells were detected in Muc2<sup>+/-</sup> and WT mice (Fig. 1B). These observations confirm the Muc2 mutation phenotype in the ileal region of the intestine.

### Increased Epithelial Cell Proliferation Is Observed in Muc2<sup>-/-</sup> but not Muc2<sup>+/-</sup> Mice

Muc2<sup>-/-</sup> mice developed colitis after about 4 weeks, but the ileum lacked any signs of mucosal damage, such as superficial erosions. In the ileum, there were no apparent differences in overall morphology of the epithelium in Muc2<sup>-/-</sup>, Muc2<sup>+/-</sup>, and WT mice at 2 weeks but from 4 weeks the villi of Muc2<sup>-/-</sup> mice were significantly ( $P < 0.05$ ) longer (but not the crypts) ( $260 \pm 6.6 \mu\text{m}$

compared with WT and Muc2<sup>+/-</sup>,  $200 \pm 6.2 \mu\text{m}$ ) (Fig. 2A). Ki67-staining revealed epithelial hyperproliferation in ileal crypts of Muc2<sup>-/-</sup> compared with WT mice at week 2 (Fig. 2B). There were no apparent differences in numbers of caspase 3-stained epithelial cells in ileum from Muc2<sup>-/-</sup> and WT mice (Fig. 2B). Taken together, this indicates that the elongated villi observed at weeks 4 and 8 in Muc2<sup>-/-</sup> mice were due to increased epithelial cell proliferation.

### Muc2 Limits Contact of Bacteria with Ileal Epithelium

As the mucus barrier has been proposed to play a role in restricting direct contact between the microbiota and the mucosa, we stained bacteria in situ using fluorescence in situ hybridization and measuring the average distance between bacterial cells and the mucosal surface. In WT mice, a distance of approximately 50  $\mu\text{m}$  was measured between the microbiota and the top of the ileal villi (Fig. 3A), corresponding to the thickness and position of the mucus layer in healthy Carnoy's-fixed ileal tissue (not shown). In the ileum of Muc2<sup>-/-</sup> mice, the microbiota are more frequently observed in contact with epithelial surfaces than in WT (Fig. 3B), confirming the microbiota barrier function of Muc2 in the ileum.

### Mucus Plays a Role in Shaping the Microbiota Composition, Diversity, and Richness

To investigate the impact of Muc2-deficiency on the colonization pattern of the ileum, 16S DNA microbiota profiles of ileal content from 4- and 8-week-old WT, Muc2<sup>+/-</sup>, and Muc2<sup>-/-</sup> mice were determined using the MITChip microarray.<sup>29</sup> At 4 weeks, the ileal content of Muc2<sup>-/-</sup> mice displayed a significantly higher microbial diversity than WT mice ( $P < 0.05$ ) because of increased richness in bacterial taxonomic units (Fig. 4A, B). The richness of the microbiota samples from Muc2<sup>+/-</sup> mice was also significantly higher than WT mice at 4 weeks (Fig. 4B). However, at week 8, the microbiota diversity and richness was similar in all groups of mice (Fig. 4B). Nevertheless, redundancy analysis clearly established that both at weeks 4 and 8, the microbiota composition clustered according to the host's genotype (Fig. 4C, D). At week 4, the variance between microbiota of WT and other groups of mice was partly explained by higher abundance of a range of different microbial groups (Fig. 4C). This could be an indication that in WT, there is an initial colonization by a more constrained group of bacteria that reached higher abundance in the WT mice compared with the other groups of mice. In the Muc2<sup>+/-</sup> and Muc2<sup>-/-</sup> groups, however, there is only 1 genus-like group, *Bryantella* spp. that was more abundant in the Muc2<sup>-/-</sup> group (Fig. 4C). This lack of multiple microbial groups with higher abundances in the Muc2<sup>+/-</sup> and Muc2<sup>-/-</sup> mice could be an indication of colonization with a higher number of different microbial groups albeit at low relative abundance per group. The idea that Muc2<sup>+/-</sup> and Muc2<sup>-/-</sup> mice are colonized by many, low abundance species at week 4 is supported by the richness calculation showing that

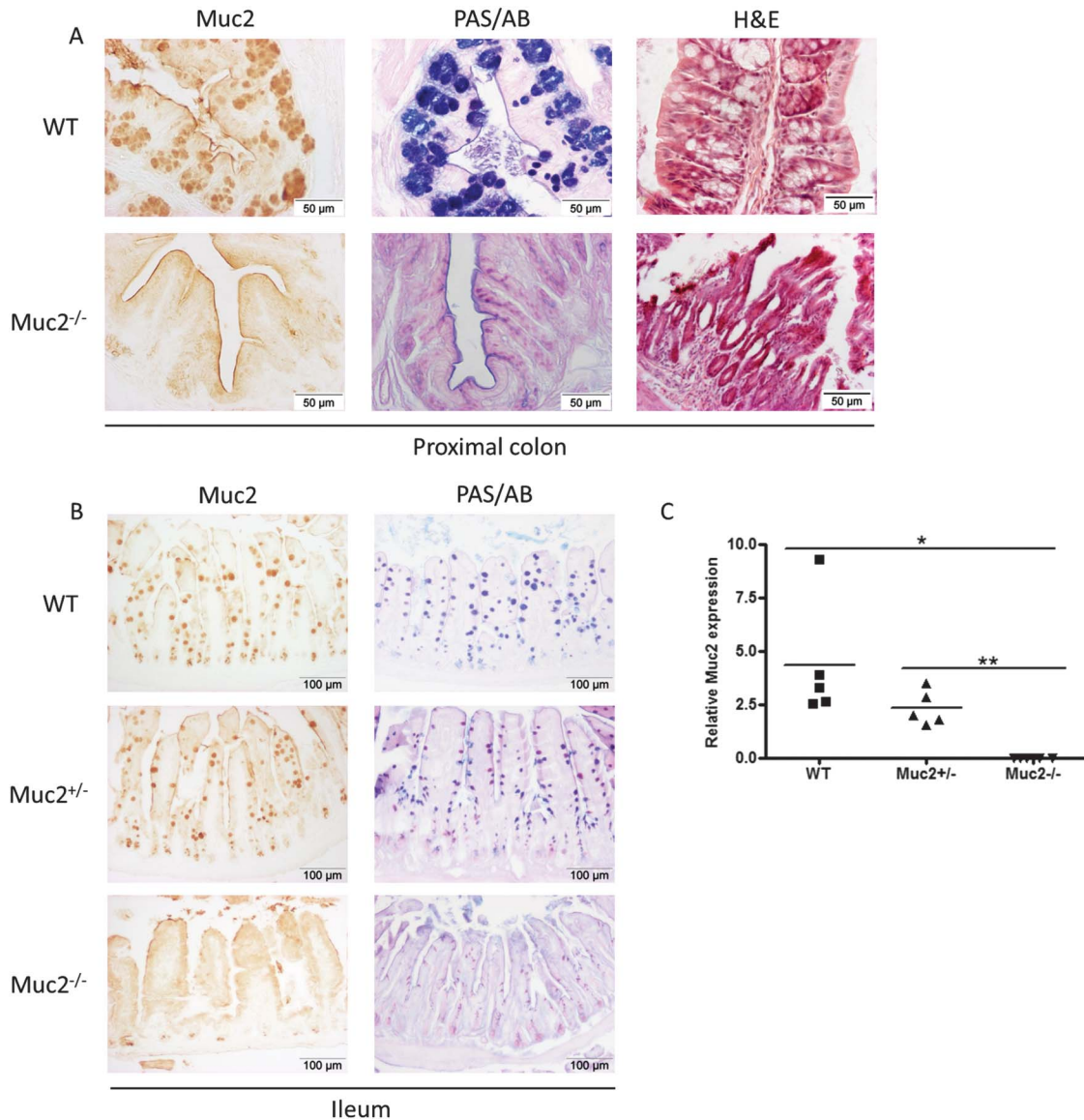


FIGURE 1. Representative pictures of H&E staining, Muc2-specific staining, and PAS/AB-staining of proximal colon of WT and Muc2<sup>-/-</sup> (A). Representative pictures of Muc2-staining and PAS/AB-staining in ileum of WT (top panels), Muc2<sup>-/-</sup> (lower panels) and heterozygote (Muc2<sup>+/-</sup>, middle panels) mice at 8 weeks of age (B). Relative Muc2 mRNA expression in the ileum determined by qPCR. \*P < 0.05, \*\*P < 0.01 (C).

Muc2<sup>+/-</sup> and Muc2<sup>-/-</sup> have higher bacterial diversity than WT mice (Fig. 4B).

In adult mice (week 8), the redundancy analysis revealed specific differences between the microbiota of WT mice and the Muc2<sup>+/-</sup> and Muc2<sup>-/-</sup> mice, which was mainly associated with higher relative abundances of *Desulfovibrio* spp, *Escherichia coli*, *L. salivarius*, and *Turicibacter* et rel in WT mice, and higher relative abundances of *Lactobacillus plantarum* et rel. and *A. muciniphila* in Muc2<sup>+/-</sup> and Muc2<sup>-/-</sup> mice (Fig. 4D). In the principal response curves over time, the microbiota community displayed more overall similarity in adult animals (week 8) as compared with those at the early weaning stage (week 4) (not shown).

### Muc2-deficiency Specifically Alters Expression of Numerous Immune, Metabolic, and Cell-cycle Control Pathways in Ileum

The number of differentially expressed genes in ileum of Muc2<sup>-/-</sup>, compared with WT, was around 10-fold higher at 4 weeks than at weeks 2 and 8. Interestingly, a similar pattern is also visible in the Muc2<sup>+/-</sup> mice, although at week 4, the number of differentially regulated genes was less than in the Muc2<sup>-/-</sup> (not shown).

GSEA, using the differentially expressed ileal genes as input, was used to identify significantly modulated gene networks in the different genotypes. In the ileum of Muc2<sup>-/-</sup> mice, specific immune-related gene sets were repressed at weeks 2, 4, and 8

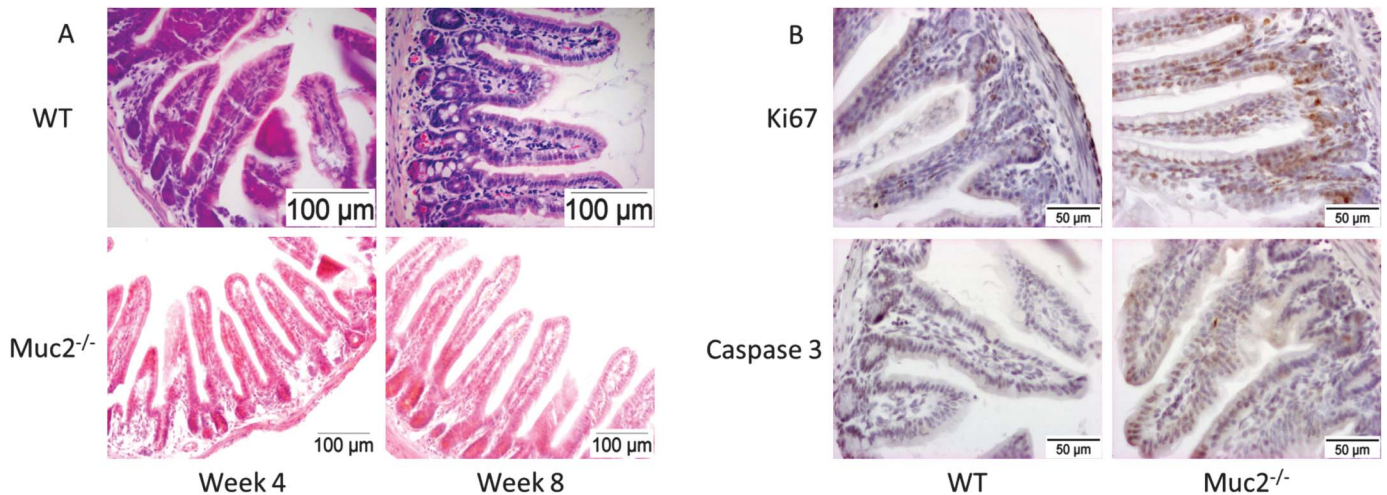


FIGURE 2. H&E staining of ileum of WT and *Muc2*<sup>-/-</sup> mice at 4 weeks and 8 weeks of age (A). Ki67 and Caspase 3 staining of ileum in WT and *Muc2*<sup>-/-</sup> mice (B).

compared with their WT counterparts, including Toll-like receptor-, immune-, and chemokine-signalling (Fig. 5A, B). Conversely, gene sets involved in mitosis, cell-cycle control, and oxidative phosphorylation were induced in *Muc2*<sup>-/-</sup> compared with WT mice at all time points (Fig. 5A, B). Notably, at week 8, but not week 4, adaptive immune response pathways were repressed in *Muc2*<sup>-/-</sup> mice compared with wild-type mice (Fig. 6B). At both weeks 4 and 8, lipid metabolism pathways were repressed in *Muc2*<sup>-/-</sup> (Fig. 5A, B).

Further analysis using Ingenuity highlighted that the highest upregulated genes at week 2 were Fucosyltransferase 2 (*Fut2*), Metalloproteinase-7 (*Mmp7*), and Reg3γ. Later on, Serum Amyloid A1 (*Saa1*), Fucosyltransferase 2 (*Fut2*), and Resistin-like β (*Relmb*), Beta-1,3-galactosyltransferase 5 (*B3Galt5*), and the IL-22-induced proliferative gene *Pla2g5* were the highest significantly increased genes in *Muc2*<sup>-/-</sup> at weeks 4 and 8 (not shown).

To gain more insights into the processes affected in the heterozygote *Muc2*<sup>+/-</sup> mice compared with the WT, we also performed GSEA to identify the most significantly affected processes (Fig. 5C, D), although *Muc2*<sup>+/-</sup> and *Muc2*<sup>-/-</sup> mice appeared to have many differentially expressed genes in common. For example, gene sets associated with cell cycle and metabolic functions were consistently upregulated and downregulated, respectively, in both the *Muc2*<sup>+/-</sup> and *Muc2*<sup>-/-</sup> mice compared with the WT at each time point. However, comparative analysis identified considerable differences between the *Muc2*<sup>+/-</sup> and *Muc2*<sup>-/-</sup> mice in comparison with the WT, which was clearly exemplified by the immune system-related gene sets that were upregulated at all time points in the *Muc2*<sup>+/-</sup> compared with the WT, whereas they were consistently downregulated in the *Muc2*<sup>-/-</sup> relative to the WT (Fig. 5). Interestingly, the heterozygote mice also significantly overexpressed (but with lower fold changes) the genes that were

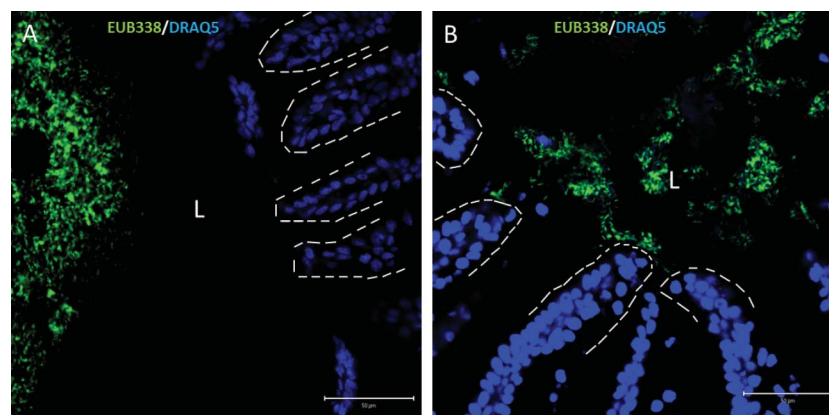


FIGURE 3. Fluorescence in situ hybridization analysis of the distal ileum of WT (A) and *Muc2*<sup>-/-</sup> (B) using the general bacterial probe EUB338-Alexa Fluor 488 (green) and nuclei staining DRAQ5 (blue). The apical membranes of the epithelial cells are indicated by a dashed white line. Scale bar, 50 μm; L indicates lumen.

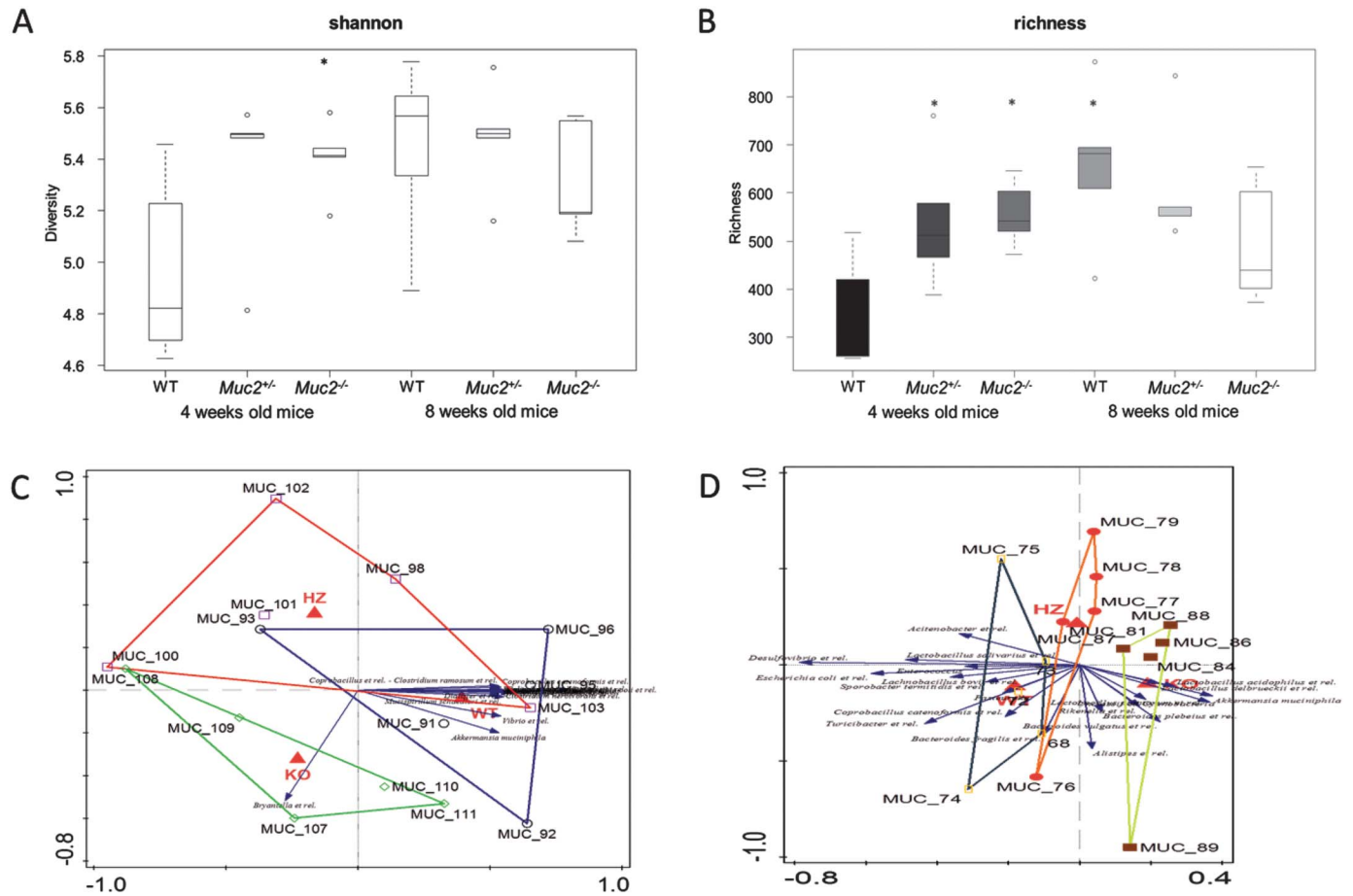


FIGURE 4. Box and whiskers plot showing the diversity (Shannon index) of microbiota in ileum of WT, *Muc2*<sup>+/-</sup>, and *Muc2*<sup>-/-</sup> mice (A). Box and whiskers plot showing the richness of microbiota in ileum of WT, *Muc2*<sup>+/-</sup>, and *Muc2*<sup>-/-</sup> mice (B). Redundancy analysis representing microbial ecology of *Muc2*<sup>-/-</sup>, *Muc2*<sup>+/-</sup>, and WT in the ileum at weeks 4 (C) and 8 (D).

expressed at the highest fold-change levels in the *Muc2*<sup>-/-</sup> mice at weeks 4 and 8, such as *Saa1*, *Fut2*, and *Relmb* (not shown).

Additionally, to confirm the data observed in the transcriptomic analysis, qPCR were done on specific genes involved in inflammation (*IL-1β*), innate immunity (*Reg3β* and *Reg3γ*), and fucosylation (*Fut2*). We showed that *Reg3β* and *Reg3γ* mRNA levels were significantly increased in *Muc2*<sup>-/-</sup> at weeks 8, compared with WT and *Muc2*<sup>+/-</sup> (Fig. 6A, B). *Fut2* mRNA levels were strongly increased in *Muc2*<sup>-/-</sup> at weeks 4 and 8 (Fig. 6C). *IL-1β* mRNA levels were not significantly different in any of the groups at week 8 (Fig. 6D). Those data are in line with the transcriptomics data previously described.

### IL-22 Pathway Plays a Key Role in Maintaining the Homeostasis in the Ileum of *Muc2*<sup>-/-</sup> Mice

The IPA Upstream Regulator Analysis enabled us to identify the cascade of upstream transcriptional regulators that can explain the observed gene expression changes in the ileum of *Muc2*<sup>-/-</sup> mice. Many upstream transcriptional regulators were activated or inhibited in *Muc2*<sup>-/-</sup> mice at each time point, although only a few were connected to immune responses.

Among the upstream regulators, IL-22 was identified as playing a central role in the activation of gene expression at weeks 2 and 4 in the *Muc2*<sup>-/-</sup> mice (Fig. 7). Notably, IL-22 is produced by activated DCs and type 3 subset of innate lymphoid cells after sensing bacteria and initiates protective innate immune responses against bacterial pathogens especially in epithelial cells.<sup>33</sup> Therefore, increased IL-22 signalling could explain the upregulation of innate immunity-related genes like *Reg3γ*, *Saa1*, *Fut2*, and *Relmb* at weeks 2 and 4 in *Muc2*<sup>-/-</sup> mice (Fig. 7). This is consistent with our finding that expression of IL-22ra2, a secreted soluble antagonist of IL-22 signalling was decreased in *Muc2*<sup>-/-</sup> mice. Moreover, proliferative factors, such as *Myc*, were also potentially controlled by the IL-22 signalling pathway at week 2 in the *Muc2*<sup>-/-</sup> mice, which correlates with the observed hyperproliferation (Ki67-positive cells) at this time point.

### DISCUSSION

*Muc2* is the major secreted intestinal mucin and in its absence was previously shown to cause colitis in mice.<sup>16,17</sup> We



FIGURE 5. Network representation of GSEA profile of upregulated (red) or downregulated (blue) pathways in the ileum of *Muc2*<sup>-/-</sup> mice compared with WT mice at weeks 4 (A) and week 8 (B). Network representation of GSEA profile of upregulated (red) or downregulated (blue) pathways in the ileum of *Muc2*<sup>+/-</sup> mice compared with WT mice at weeks 4 (C) and 8 (D). The “geography” of these representations has no implicit meaning.

confirmed that after 4 weeks, *Muc2*<sup>-/-</sup> mice develop colitis evidenced by increased thickness of the mucosa associated with hyperproliferation, apoptosis in crypts, ulceration accompanied by fecal blood, and weight loss.<sup>16,17</sup> These histological changes are characteristic of murine models for IBD and clinical symptoms of IBD in humans. To date, the effect of *Muc2*<sup>-/-</sup> or *Muc2*<sup>+/-</sup> genotypes on small intestinal physiology and microbiota have not been described in detail. Therefore, our aim was to investigate

how the small intestine responds to complete (*Muc2*<sup>-/-</sup>) or partial (*Muc2*<sup>+/-</sup>) mucus-barrier defects as it might reveal crucial differences in ileal homeostatic mechanisms.

Deletion of *Muc2* was not compensated by expression of other secreted mucins *Muc5B*, *Muc5AC*, or *Muc6* in the ileum (results not shown). In contrast to the colon, the ileum of *Muc2*<sup>-/-</sup> showed no histological signs of tissue damage, the only noticeable morphological difference being an increased length of



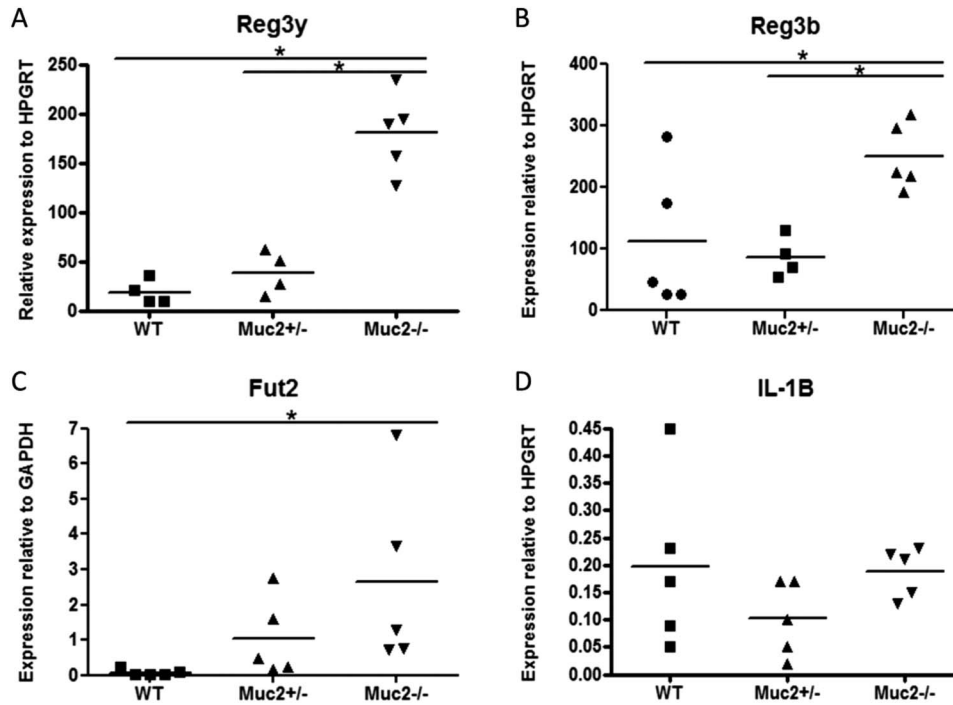


FIGURE 6. Quantitative PCR measurements of Reg3 $\gamma$  (A), Reg3 $\beta$  (B), Fut2 (C), and IL-1 $\beta$  (D) in ileum of WT, Muc2<sup>+/-</sup> and Muc2<sup>-/-</sup> mice at week 8. \**P* < 0.05.

the villi (weeks 4 and 8) in agreement with our results showing hyperproliferation of the intestinal epithelium. The evidence for hyperproliferation comes from increased epithelial staining of Ki-67 but not apoptotic cells, as well as increased expression of genes involved in cell-cycle progression and differentiation, such as *Myc* and *Pla2g5*, were observed in Muc2<sup>-/-</sup> mice (week 2).

Few genes associated with inflammation, such as *Mip-1a* (*Ccl3*), *Tnf- $\alpha$* , and *Ccl17* were upregulated in ileum of Muc2<sup>-/-</sup> compared with WT. Eight genes of the mouse orthologs of human IBD-related genes,<sup>34</sup> i.e., IL6ra, IL22ra1, *Ccl2*, *Cxcl1*, *Timp1*,

*S100a6*, *S100a13*, and *Abcb1a* were differentially expressed. In contrast, 12 of the 32 IBD-related genes were upregulated in colon of both Muc2<sup>-/-</sup> and Muc2<sup>+/-</sup> mice at weeks 4 and 8 (not shown). Interestingly, one of the strongly downregulated genes in the ileum was *Tlr5*, which induces NF- $\kappa$ B activation upon binding of bacterial flagellin. Indeed, downregulation of *Tlr5* in colitis has been observed and may be a feedback response to low-level inflammation.<sup>35</sup> Furthermore *Nfap*, a transcriptional activator of NF- $\kappa$ B, was downregulated, whereas *I $\kappa$ B*, an NF- $\kappa$ B inhibitor that binds to cytosolic NF- $\kappa$ B to prevent nuclear

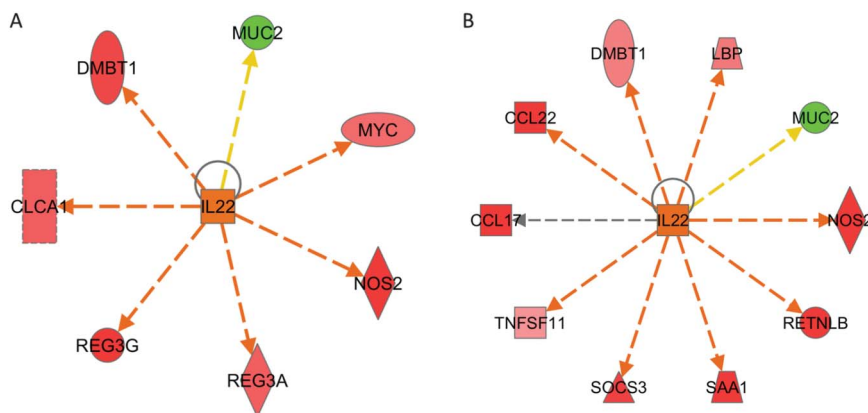


FIGURE 7. Downstream genes regulated by IL-22 in the ileum of Muc2<sup>-/-</sup> mice at week 2 (A) and week 4 (B). Upregulated genes are depicted in shades of red and downregulated are indicated in green. The color of the arrow indicates the influence of IL-22 on the respective genes. Brown arrows indicate activation of the gene, yellow arrows indicate that the findings are not consistent with state of downstream molecule, and gray arrows indicate that the effect is not predicted.

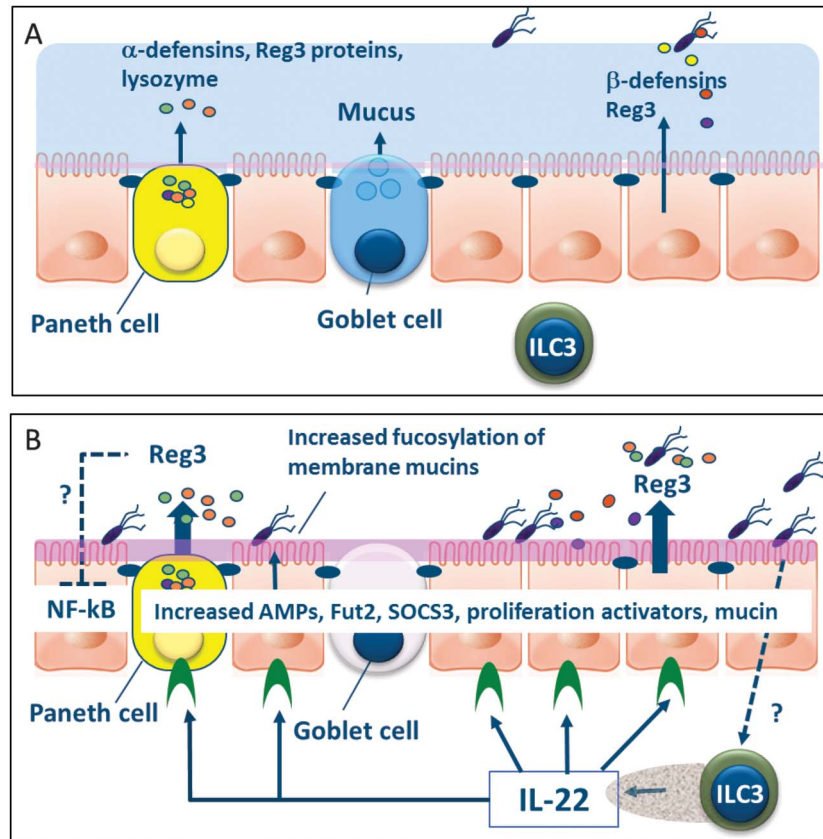


FIGURE 8. The IL-22-STAT3 pathway plays a key role in the maintenance of ileal homeostasis in *Muc2*-deficient mice. A, Schematic representation of the small intestine of a WT mouse. B, Schematic representation of the small intestine of *Muc2*<sup>-/-</sup> mice showing known functions of IL-22. The anti-inflammatory mechanism of PAP (Reg3 $\beta$ ) on NF- $\kappa$ B-driven inflammatory pathways is shown as a dotted line as it has only been described for human colonic tissue and the precise mechanisms are not known. We speculate that IL-22 might also regulate FUT2 (shown as a dotted line). Mucus is indicated in blue, fucosylation is indicated in pink. IEL, intraepithelial lymphocytes; AMPs, antimicrobial peptides; SOCS3, suppressor of cytokine signalling 3.

translocation, was among the most strongly upregulated genes. This apparent repression of innate inflammatory signalling through repression of NF- $\kappa$ B signalling may have contributed to preventing immune-mediated pathology in ileal mucosa of *Muc2*<sup>-/-</sup>. In contrast, innate defense genes encoding antimicrobial Defb46, Reg3 $\beta$ , and Reg3 $\gamma$  were expressed at significantly greater amounts in *Muc2*<sup>-/-</sup> than in WT mice.

In contrast to WT, bacteria in the ileum of *Muc2*<sup>-/-</sup> mice were frequently found in direct contact with the epithelium. However, the expression of innate gene sets except for Reg3 and defensins was less in the *Muc2*<sup>-/-</sup> mice than in WT, given the results of our extensive GSEA analysis. This supports the notion that innate responses were suppressed in the ileum of *Muc2*<sup>-/-</sup> mice compared with WT, possibly through a regulatory feedback mechanism. One plausible explanation for reduced expression of innate pathway genes could be the relatively high amounts of Reg3 $\gamma$  and Reg3 $\beta$  expressed in the *Muc2*<sup>-/-</sup> mice. Incubation of mucosa from active Crohn's disease with the human ortholog of Reg3 $\beta$  (HIP/PAP) was shown to reduce proinflammatory cytokines secretion.<sup>36</sup> Furthermore, PAP prevented TNF- $\alpha$ -induced

NF- $\kappa$ B activation in monocytic, epithelial, and endothelial cells and reduced proinflammatory cytokine mRNA levels and adhesion molecule expression.<sup>36</sup> Moreover, antisense blocking of PAP expression in a rat model of acute pancreatitis increases severity of inflammation.<sup>37</sup> In endothelial cells, purified human HIP/PAP decreased expression of surface receptors involved in leukocyte recruitment suggesting that HIP/PAP might dampen inflammatory responses by inhibiting leukocyte recruitment into the intestine.<sup>36</sup>

These findings support the idea that Reg3 proteins have anti-inflammatory activity and their upregulation participates in protection of epithelial cells in response to excessive inflammatory stimuli. Downregulation of NF- $\kappa$ B and inflammatory pathways in the ileum of *Muc2*<sup>-/-</sup> mice, which express high amounts of Reg3 $\beta$  and Reg3 $\gamma$ , is reminiscent of the effects of IL-10, an anti-inflammatory cytokine, triggering expression of suppressor of cytokine signalling through the JAK/STAT pathway. This hypothesis is supported by previous studies showing that purified human PAP inhibits the NF- $\kappa$ B pathway through JAK/STAT signalling in epithelial cells.<sup>38</sup>

At week 8, both Reg3 genes were significantly upregulated in the ileum of Muc2<sup>-/-</sup> mice and in the ileum of Muc2<sup>+/-</sup> mice at week 4. Expression of Reg3 proteins was also increased in the colon, but the overall amount of transcription in colon was much lower, as shown previously.<sup>39</sup> Expression of Reg3 proteins is induced during infection or inflammation<sup>40</sup> and is dependent on IL-22 signalling.<sup>41</sup> This is consistent with our finding that expression of IL-22ra2, a secreted soluble antagonist of IL-22 signalling<sup>39</sup> was decreased in Muc2<sup>-/-</sup> mice. Apart from its role in stimulation of epithelial cells to produce antibacterial proteins, IL-22 regulates cellular stress response, apoptosis, and wound healing pathways in intestinal epithelial cells through the signal transducer and activator of transcription 3 (STAT3) pathway.<sup>42</sup> Notably, STAT3 activation induces expression of IL-6, which promotes epithelial survival and proliferation,<sup>43</sup> which may explain the increased proliferation and villus length in the Muc2<sup>-/-</sup> ileum. Moreover, mRNA encoding Pla2g5, which is induced by IL-22 and stimulates proliferation in intestinal epithelial cells was strongly upregulated in Muc2<sup>+/-</sup> and Muc2<sup>-/-</sup> at weeks 4 and 8. Interestingly, expression of the IL-6 receptor was also increased in ileum of Muc2<sup>+/-</sup>. Another highly upregulated gene in the ileum at weeks 4 and 8, both in Muc2<sup>+/-</sup> and Muc2<sup>-/-</sup> was *Fut2*. The *Fut2* gene, encoding an  $\alpha$ -1,2-fucosyltransferase responsible for enzymatic linkage of  $\alpha$ -1,2-linked fucose to cell membrane attached and secretory mucins of the intestinal mucosa,<sup>44</sup> was significantly upregulated in the ileum of Muc2<sup>-/-</sup> at week 8. It has been shown that at weaning, when the transition toward adult-type colonization by microbiota occurs, *Fut2* mRNA is increased leading to expression of fucosylated epitopes in the colonic epithelium and fucose decoration of mucins.<sup>45–48</sup> This may be a mechanism to promote colonization by preferred groups of symbionts that produce beneficial short-chain fatty acids and provide colonization resistance against pathogens. LP innate lymphoid cells 3 were recently shown to produce IL-22 through sensing of bacteria by an unknown mechanism<sup>33</sup> leading to increased expression of *Fut2* and Reg3 proteins. This is consistent with our observation of increased bacterial contact with the epithelium in Muc2-deficient mice (Fig. 3) and the IL-22-mediated effects on epithelial expression and proliferation reported here.

Mucus directly or indirectly played a role in shaping the microbiota composition, diversity, and richness with the greatest effect immediately preceding weaning but becoming more similar to that of WT in adult mice. This may be due to the ability of specific members of the microbiota, such as *Akkermansia muciniphila*, to colonize the mucus and use the mucus-associated glycans as a carbon source for growth.<sup>49</sup> The syntrophic interactions between mucus degraders and other bacteria in the small intestine are poorly understood, but could explain differences in composition between WT and mice lacking Muc2. The significant up-regulation of Reg3 proteins in Muc2<sup>-/-</sup> mice could also shape the composition of the microbiota through selective inhibition or killing of specific bacterial species.

In summary, we propose a key role for the IL-22/STAT3 pathway in maintaining homeostasis in the ileum as a consequence of loss of mucus barrier (Fig. 8). This model is consistent with previous studies reporting increased expression of Reg3 $\beta$  and Reg3 $\gamma$ <sup>41</sup> and stimulation of epithelial regeneration through STAT3 induction of pro-proliferative genes. For example, Pla2g5, which is induced by IL-22 and induces proliferation in intestinal epithelial cells<sup>50</sup> was strongly up-regulated in Muc2<sup>+/-</sup> and Muc2<sup>-/-</sup> mice at week 4 and 8. IL-22-induced STAT3 signalling in epithelial cells may also explain the increased expression of other protective factors such as Defb46 and Fut2. Toll-like receptor chemokine and innate pathways were down-regulation of in the ileum of Muc2<sup>-/-</sup> mice compared to WT which may be due to the protective effects of Reg3 proteins including anti-inflammatory signalling,<sup>38</sup> capacity to bind soluble microbe-associated molecular patterns and direct antimicrobial activities.<sup>51</sup> IL-22 is constitutively expressed in the small intestine by innate and adaptive cells including TCR $\gamma\delta$  T cells and DCs, which can encounter bacteria at the epithelial surface. These findings support the notion that IL-22 might be an attractive target for therapy of intestinal inflammation.

## ACKNOWLEDGMENTS

The authors are grateful to Jenny Jansen (Division of Human Nutrition, Wageningen University) for technical support in microarray hybridization, microarray data-quality control, and processing. The authors thank Steven Aalvink (Microbiology Department, Wageningen University) for his technical support in MITchip procedures. Nanda Burger-van Paassen is acknowledged for her help in the breeding of the mice and tissue acquirement.

Author contributions: B. Sovran and L. M. P. Loonen contributed equally to this study.

## REFERENCES

- Macpherson AJ, Gatto D, Sainsbury E, et al. A primitive T cell-independent mechanism of intestinal mucosal IgA responses to commensal bacteria. *Science*. 2000;288:2222–2226.
- Macpherson AJ, Harris NL. Interactions between commensal intestinal bacteria and the immune system. *Nat Rev Immunol*. 2004;4:478–485.
- Tytgat KM, Buller HA, Opdam FJ, et al. Biosynthesis of human colonic mucin: muc2 is the prominent secretory mucin. *Gastroenterology*. 1994; 107:1352–1363.
- van Klinken BJ, Einerhand AW, Duits LA, et al. Gastrointestinal expression and partial cDNA cloning of murine Muc2. *Am J Physiol*. 1999;276: G115–G124.
- Shan M, Gentile M, Yeiser JR, et al. Mucus enhances gut homeostasis and oral tolerance by delivering immunoregulatory signals. *Science*. 2013;342: 447–453.
- Johansson ME, Phillipson M, Petersson J, et al. The inner of the two Muc2 mucin-dependent mucus layers in colon is devoid of bacteria. *Proc Natl Acad Sci U S A*. 2008;105:15064–15069.
- Hansson GC. Role of mucus layers in gut infection and inflammation. *Curr Opin Microbiol*. 2012;15:57–62.
- Swidsinski A, Loening-Baucke V, Theissig F, et al. Comparative study of the intestinal mucus barrier in normal and inflamed colon. *Gut*. 2007;56:343–350.
- Tytgat KMAJ, van der Wal JWG, Einerhand AWC, et al. Quantitative analysis of MUC2 synthesis in ulcerative colitis. *Biochem Biophys Res Commun*. 1996;224:397–405.

10. Pullan RD, Thomas GA, Rhodes M, et al. Thickness of adherent mucus gel on colonic mucosa in humans and its relevance to colitis. *Gut*. 1994; 35:353–359.
11. Johansson MEV, Hansson GC. The goblet cell: a key player in ischaemia-reperfusion injury. *Gut*. 2013;62:188–189.
12. Johansson ME, Gustafsson JK, Sjöberg KE, et al. Bacteria penetrate the inner mucus layer before inflammation in the dextran sulfate colitis model. *PLoS One*. 2010;5:e12238.
13. Chow J, Tang H, Mazmanian SK. Pathobionts of the gastrointestinal microbiota and inflammatory disease. *Curr Opin Immunol*. 2011;23:473–480.
14. Abraham C, Cho JH. Mechanisms of disease inflammatory bowel disease. *N Engl J Med*. 2009;361:2066–2078.
15. Frank DN, Amand ALS, Feldman RA, et al. Molecular-phylogenetic characterization of microbial community imbalances in human inflammatory bowel diseases. *Proc Natl Acad Sci U S A*. 2007;104:13780–13785.
16. Van der Sluis M, De Koning BA, De Bruijn AC, et al. Muc2-deficient mice spontaneously develop colitis, indicating that MUC2 is critical for colonic protection. *Gastroenterology*. 2006;131:117–129.
17. Burger-van Paassen N, van der Sluis M, Bouma J, et al. Colitis development during the suckling-weaning transition in mucin Muc2-deficient mice. *Am J Physiol Gastrointest Liver Physiol*. 2011;301:G667–G678.
18. Lu P, Burger-van Paassen N, van der Sluis M, et al. Colonic gene expression patterns of mucin Muc2 knockout mice reveal various phases in colitis development. *Inflamm Bowel Dis*. 2011;17:2047–2057.
19. Velcich A, Yang W, Heyer J, et al. Colorectal cancer in mice genetically deficient in the mucin Muc2. *Science*. 2002;295:1726–1729.
20. Yamabayashi S. Periodic acid-Schiff-alcian blue: a method for the differential staining of glycoproteins. *Histochem J*. 1987;19:565–571.
21. Gentleman RC, Carey VJ, Bates DM, et al. Bioconductor: open software development for computational biology and bioinformatics. *Genome Biol*. 2004;5:R80.
22. Lin K, Kools H, de Groot PJ, et al. MADMAX—management and analysis database for multiple -omics experiments. *J Integr Bioinform*. 2011;8:160.
23. Dai M, Wang P, Boyd AD, et al. Evolving gene/transcript definitions significantly alter the interpretation of GeneChip data. *Nucleic Acids Res*. 2005;33:e175.
24. Bolstad BM, Collin F, Simpson KM, et al. Experimental design and low-level analysis of microarray data. *Int Rev Neurobiol*. 2004;60:25–58.
25. Storey JD, Tibshirani R. Statistical significance for genomewide studies. *Proc Natl Acad Sci U S A*. 2003;100:9440–9445.
26. Sartor MA, Tomlinson CR, Wesselkamper SC, et al. Intensity-based hierarchical bayes method improves testing for differentially expressed genes in microarray experiments. *BMC Bioinformatics*. 2006;7:538.
27. Subramanian A, Tamayo P, Mootha VK, et al. Gene set enrichment analysis: a knowledge-based approach for interpreting genome-wide expression profiles. *Proc Natl Acad Sci U S A*. 2005;102:15545–15550.
28. Mootha VK, Lindgren CM, Eriksson KF, et al. PGC-1 $\alpha$ -responsive genes involved in oxidative phosphorylation are coordinately downregulated in human diabetes. *Nat Genet*. 2003;34:267–273.
29. Geurts L, Lazarevic V, Derrien M, et al. Altered gut microbiota and endocannabinoid system tone in obese and diabetic leptin-resistant mice: impact on apelin regulation in adipose tissue. *Front Microbiol*. 2011;2:149.
30. Rajilic-Stojanovic M, Heilig HG, Molenaar D, et al. Development and application of the human intestinal tract chip, a phylogenetic microarray: analysis of universally conserved phylotypes in the abundant microbiota of young and elderly adults. *Environ Microbiol*. 2009;11:1736–1751.
31. Lahti L, Elo LL, Aittokallio T, et al. Probabilistic analysis of probe reliability in differential gene expression studies with short oligonucleotide arrays. *IEEE/ACM Trans Comput Biol Bioinform*. 2011;8:217–225.
32. Braak CJF, Šmilauer P. *Canoco Reference Manual and User's Guide: Software for Ordination (Version 5.0)*. Ithaca, NY: NH; 2012.
33. Goto Y, Obata T, Kunisawa J, et al. Innate lymphoid cells regulate intestinal epithelial cell glycosylation. *Science*. 2014;345:1254009.
34. te Velde AA, de Kort F, Sterrenburg E, et al. Comparative analysis of colonic gene expression of three experimental colitis models mimicking inflammatory bowel disease. *Inflamm Bowel Dis*. 2007;13:325–330.
35. Ortega-Cava CF, Ishihara S, Rumi MAK, et al. Epithelial toll-like receptor 5 is constitutively localized in the mouse cecum and exhibits distinctive down-regulation during experimental colitis. *Clin Vaccine Immunol*. 2006;13:132–138.
36. Gironella M, Iovanna JL, Sans M, et al. Anti-inflammatory effects of pancreatitis associated protein in inflammatory bowel disease. *Gut*. 2005;54:1244–1253.
37. Zhang H, Kandil E, Lin YY, et al. Targeted inhibition of gene expression of pancreatitis-associated proteins exacerbates the severity of acute pancreatitis in rats. *Scand J Gastroenterol*. 2004;39:870–881.
38. Closa D, Motoo Y, Iovanna JL. Pancreatitis-associated protein: from a lectin to an anti-inflammatory cytokine. *World J Gastroenterol*. 2007; 13:170–174.
39. Xu W, Presnell SR, Parrish-Novak J, et al. A soluble class II cytokine receptor, IL-22RA2, is a naturally occurring IL-22 antagonist. *Proc Natl Acad Sci U S A*. 2001;98:9511–9516.
40. van Ampting MT, Loonen LM, Schonewille AJ, et al. Intestinally secreted C-type lectin Reg3b attenuates salmonellosis but not listeriosis in mice. *Infect Immun*. 2012;80:1115–1120.
41. Zheng Y, Valdez PA, Danilenko DM, et al. Interleukin-22 mediates early host defense against attaching and effacing bacterial pathogens. *Nat Med*. 2008;14:282–289.
42. Pickert G, Neufert C, Leppkes M, et al. STAT3 links IL-22 signaling in intestinal epithelial cells to mucosal wound healing. *J Exp Med*. 2009;206: 1465–1472.
43. Grivnickov S, Karin E, Terzic J, et al. IL-6 and Stat3 are required for survival of intestinal epithelial cells and development of colitis-associated cancer. *Cancer Cell*. 2009;15:103–113.
44. Meng D, Newburg DS, Young C, et al. Bacterial symbionts induce a FUT2-dependent fucosylated niche on colonic epithelium via ERK and JNK signaling. *Am J Physiol Gastrointest Liver Physiol*. 2007;293: G780–G787.
45. Bry L, Falk PG, Midtvedt T, et al. A model of host-microbial interactions in an open mammalian ecosystem. *Science*. 1996;273: 1380–1383.
46. Nanthakumar NN, Dai D, Newburg DS, et al. The role of indigenous microflora in the development of murine intestinal fucosyl- and sialyl-transferases. *FASEB J*. 2003;17:44–46.
47. Pang KY, Newman AP, Udall JN, et al. Development of gastrointestinal mucosal barrier. VII. In utero maturation of microvillus surface by cortisone. *Am J Physiol*. 1985;249:G85–91.
48. Shub MD, Pang KY, Swann DA, et al. Age-related changes in chemical composition and physical properties of mucus glycoproteins from rat small intestine. *Biochem J*. 1983;215:405–411.
49. Derrien M, Collado MC, Ben-Amor K, et al. The Mucin degrader Akkermansia muciniphila is an abundant resident of the human intestinal tract. *Appl Environ Microbiol*. 2008;74:1646–1648.
50. Neufert C, Pickert G, Zheng Y, et al. Activation of epithelial STAT3 regulates intestinal homeostasis. *Cell Cycle*. 2010;9:652–655.
51. Cash HL, Whitham CV, Hooper LV. Refolding, purification, and characterization of human and murine RegIII proteins expressed in Escherichia coli. *Protein Expr Purif*. 2006;48:151–159.